



Cite this: *Phys. Chem. Chem. Phys.*, 2016, 18, 1397

Received 29th August 2015,  
Accepted 1st December 2015

DOI: 10.1039/c5cp05171a

www.rsc.org/pccp

## Thiolated Au<sub>18</sub> cluster: preferred Ag sites for doping, structures, and optical and chiroptical properties†

Bertha Molina<sup>a</sup> and Alfredo Tlahuice-Flores<sup>\*b</sup>

Recently, the X-ray determined structure of the thiolated Au<sub>18</sub> cluster has been reported. In this communication, we addressed a study of structures and chiroptical properties of thiolated Au<sub>18</sub> cluster doped with up to ten Ag atoms, which have been calculated by Time Dependent Density Functional Theory (TD-DFT). The number of Ag atoms was steadily varied and more stable isomers showed optical and Circular Dichroism (CD) spectra distinct from that found for the parent Au<sub>18</sub> cluster. Doping with more than four Ag atoms results in enhancement of the oscillator strength of the HOMO–LUMO peak and it is expected that this feature can be exploited for photoluminescence applications.

The doping of thiolated gold clusters has captured our interest since the first experimental report of Pd doping of the anionic Au<sub>25</sub>(SR)<sub>18</sub> cluster<sup>1</sup> by Murray's group in 2009.<sup>2</sup> In the amply studied thiolated Au<sub>25</sub> cluster, the preferred site for doping depends on the atom; for example, Pd and Pt atoms prefer inner positions,<sup>3,4</sup> Mn and Ag are located at the surface of the core,<sup>3c,5–9</sup> while Cu and Hg were found at staple-like motifs by experimental groups.<sup>10</sup> It can be noted that the radii of Ag and Au atoms are similar, allowing their mixing; in contrast, doping using Cu atoms might introduce more distortion into the structure. Recently, new alloys have been reported for thiolated Au<sub>144</sub>,<sup>11</sup> Au<sub>130</sub><sup>12</sup> and Au<sub>38</sub> clusters.<sup>13</sup>

Ultrasmall bimetallic thiolate-protected clusters, in the case of Au<sub>24</sub>Pd(SR)<sub>18</sub> and Au<sub>36</sub>Pd<sub>2</sub>(SR)<sub>24</sub>, are significantly more stable against degradation in a solution, laser dissociation and core etching by thiol.<sup>14</sup> In addition, they display molecular-like

properties and the incorporation of two types of metal atoms is reported to enhance their photoluminescence;<sup>7e</sup> moreover, their properties could be tailored by controlling their compositions.<sup>7b</sup> Potential applications of bimetallic thiolated clusters include catalysis<sup>15</sup> and bio-sensors.<sup>16</sup>

Regarding the smallest bimetallic cluster, an experimental study by Pradeep *et al.*<sup>17</sup> and a theoretical study by Tlahuice-Flores in 2014 have revealed the structure of the Au<sub>6</sub>Ag<sub>7</sub>(SR)<sub>13</sub> cluster as an octahedral-like Ag<sub>6</sub> core protected by two dimers and one Au<sub>2</sub>Ag(SR)<sub>4</sub> motif.<sup>18</sup> Thus, both Ag<sub>6</sub>Au<sub>7</sub> and Au<sub>25</sub><sup>8</sup> clusters show a clear preference to incorporate Ag atoms into their core, and their frontier (HOMO and LUMO) levels have contribution from Ag and S atoms. Therefore, the electronic excitations are influenced by foreign atoms, which are incorporated into the monometallic clusters.

Thiolated Au<sub>15</sub> and Au<sub>18</sub> clusters are important systems because they have been devised as the smallest thiolated gold clusters with two and four electrons, respectively. The thiolated Au<sub>15</sub> cluster model has been reported and it was proposed as a Au<sub>4</sub> core protected by two trimer motifs plus a closed pentameric [SR–Au]<sub>5</sub> ring<sup>19</sup> or protected by one heptamer and one tetramer motif.<sup>20</sup> The latter model of the thiolated Au<sub>15</sub> cluster was proposed based on the superior agreement between the calculated CD spectrum featuring a prominent negative peak located at 3.48 eV and the experimental 3.42 eV band.<sup>20</sup> Following this line, experimental work devoted to the elucidation of the structure of thiolated Au<sub>18</sub> cluster succeeded recently<sup>21</sup> in providing theoretical groups<sup>22</sup> the opportunity to correct their algorithms used to propose structures and to improve our knowledge in this field.

Herein, a DFT<sup>23</sup> study of the X-ray determined structure of thiolated Au<sub>18</sub> cluster produced by doping with up to ten Ag atoms is addressed.<sup>21b</sup> The aim of this study is to determinate how the structure, the HOMO–LUMO (HL) gap values, the oscillator strength of the lower energy peak, and the optical and chiroptical properties are affected by Ag doping. A systematic search of lowest-energy isomers was carried out using the PBE functional<sup>24</sup> for the exchange and correlation (XC) terms.

<sup>a</sup> Facultad de Ciencias, Universidad Nacional Autónoma de México, Apartado Postal 70-646, 04510 México D.F., Mexico

<sup>b</sup> CICFIM-Facultad de Ciencias Físico-Matemáticas, Universidad Autónoma de Nuevo León, San Nicolás de los Garza, NL 66450, Mexico.  
E-mail: tlahuicef@gmail.com

† Electronic supplementary information (ESI) available: Comparison between calculated and experimental absorption spectrum of thiolated Au<sub>18</sub>, an extended set of studied structures and a table with Boltzmann weights and with electronic excitations and their oscillator strengths, and Cartesian coordinates of more stable isomers are provided. See DOI: 10.1039/c5cp05171a

The Slater type basis sets employed in the geometry optimizations are of polarized triple (TZP) quality with a  $[1s^2-4f^{14}]$  frozen core for Au, a  $[1s^2-2p^6]$  frozen core for S, and a  $[1s^2]$  frozen core for C. The energy convergence criterion is tightened to  $10^{-5}$  Hartree, and the gradient convergence criterion is tightened to  $10^{-4}$  Hartree per Å. Scalar relativistic effects were included through the Zeroth Order Regular Approximation (ZORA).<sup>25</sup> Time-dependent DFT, as implemented in the ADF package, was utilized for the study of the optical and chiroptical properties, through the calculation of its excitation energies and oscillator and rotatory strengths.<sup>26</sup> To calculate the optical absorption and circular dichroism spectra, particularly in the low energy region (0.5–4.0 eV), the lowest 300 excited (singlet) states were considered, using the same XC functional and basis set as for the structural calculations. To test the reliability of the present TD-DFT methodology, a comparison between the calculated optical absorption spectrum of the  $\text{Au}_{18}(\text{SCH}_3)_{14}$  cluster and the experimental data was carried out, indicating good agreement, as shown in the ESI† (Fig. S1).

The thiolated  $\text{Au}_{18}$  cluster itself is a red-emitting cluster,<sup>27</sup> which is built by one  $\text{Au}_9$  core that resembles two octahedral-like clusters linked by a shared triangular face (STF) and covered with three monomer motifs located around an axis perpendicular to the STF, while one dimer and one tetramer motifs are located at the ends of the  $\text{Au}_9$  core. There exists one special position where one Au atom is linked to both one monomer and one dimer motif. Previously, we reported an isomer constituted by one  $\text{Au}_8$  core that was described as a bi-capped octahedral-like cluster, while the structure reported here can be seen as a tri-capped octahedral-like cluster.<sup>22</sup> Fig. 1 depicts the arrangement of staple-like motifs in the optimized structure that holds a 1.48 eV HL gap value. Moreover, calculated Au–Au distances in the  $\text{Au}_9$  core (from 2.72 to 3.00 Å) are in agreement with those reported in ref. 21b (from 2.67 to 3.00 Å). The distances in the staple-like motifs are calculated as 1.84 Å (S–C) and 2.34–2.37 Å for Au–S bonds. Bonds between an Au core and Au adatoms are comparable to Au–Au bonds in the  $\text{Au}_9$  core. Thus, we can conclude that the interaction between the  $\text{Au}_9$  core and staple-like motifs is strong due to the compact structure. A complete graph of calculated bond lengths is included in the ESI† (Fig. S2).

In order to study the effect of the Ag doping in the structure of the thiolated  $\text{Au}_{18}$  cluster, a set of clusters was explored by

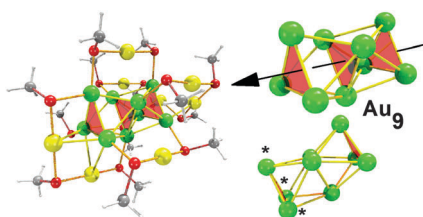


Fig. 1 Structure of the optimized  $\text{Au}_{18}(\text{SCH}_3)_{14}$  cluster. The Au, S, C, and H atoms are yellow, red, gray and white, respectively. The arrow indicates an axis along the  $\text{Au}_9$  core that is displayed in green color, where the middle triangular face is shared by two octahedral-like units. In addition, the  $\text{Au}_9$  core can be described as a tri-capped (indicated with asterisks) octahedral-like cluster (right and bottom figures).

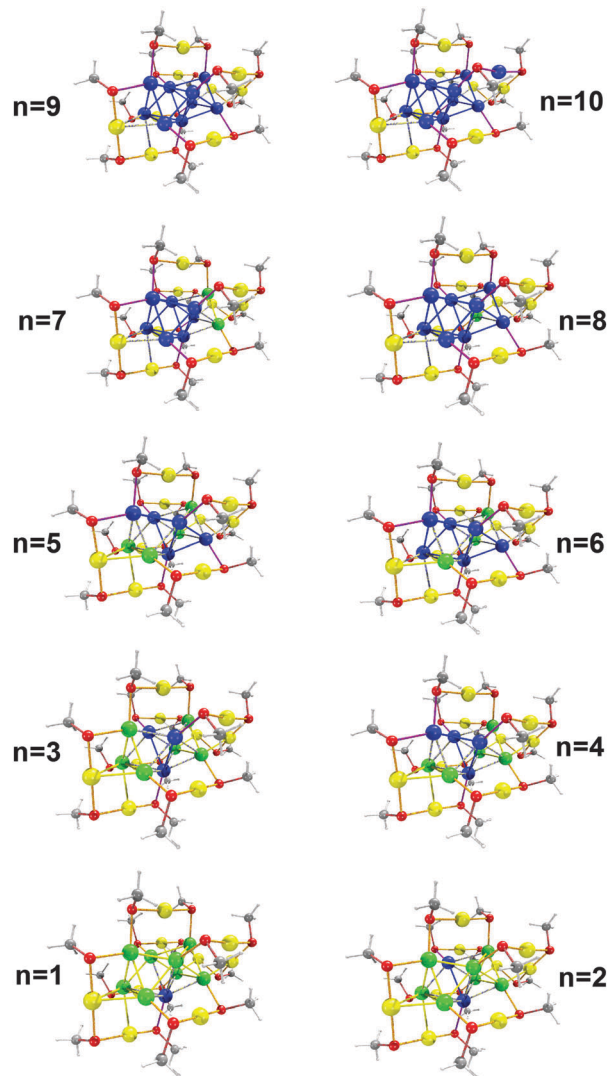


Fig. 2 More stable isomers with up to ten Ag atoms ( $n = 1$ –10) doping the parent  $\text{Au}_{18}$  cluster. It is found that an isomer with a relative energy of 0.26 eV contains five Ag atoms in the inner core and cluster. Colors are same as indicated in Fig. 1, but Ag atoms are shown in blue.

varying the position and number of Ag atoms (given by  $n$ ). Starting from one Ag doping atom, a large set of isomers was obtained by testing positions in both the  $\text{Au}_9$  core and the staple-like motifs. After a normal modes analysis, representative low-energy isomers, for each composition, were selected and they are displayed in Fig. 2. Furthermore, a more complete set of isomers for each  $n$  is provided in Table S1 (ESI†).

An interesting subject is to determinate possible sites of doping as a function of the number of Ag atoms incorporated into the parent  $\text{Au}_{18}$  cluster. Mathematically, the number of isomers (NH) for each composition of Au–Ag bimetallic cluster is given as follows:

$$\text{NH} = N!/(n!(N - n)!)$$

where  $N$  is the total number of gold atoms and  $n$  is the number of incorporated silver atoms.

It is important to mention that we reduced the large number of isomers for a composition of  $n + 1$  Ag atoms by exploring positions close to the favoured sites from previous compositions ( $n$ ). For example, we maintained the lower energy isomer for  $n = 4$  and played with the rest of the positions to generate a set of isomers for  $n = 5$ . Moreover, we double checked the trend to verify whether the trend was maintained for large values of  $n$ ; for example, for  $n = 7$ , we relaxed a total of 23 isomers.

Our results regarding Ag doping can be summarized as follows:

(1) We relaxed a set of 18 isomers for mono-substitution of Ag atoms. The preferred Ag doping is found to occur in the Au<sub>9</sub> core rather than in the staple-like motifs. The energy minimum is obtained when one Ag atom is located at one core atom linked to one terminal S atom of the dimer motif (1.59 eV HL gap value and Ag–S of 2.59 Å). It was found that the Ag atom linked to a terminal S atom of the dimer motif is larger than Au–S bonds by *circa* 0.05 Å. However, when one core Ag atom is linked to the tetramer motif, the cluster is 59.3 meV close in energy. The preference for Ag doping is found as follows: core atoms (0.0–0.15 eV) > monomer (0.16–0.24 eV) > tetramer (0.19–0.22 eV) > dimer motifs (0.25–0.26 eV). The less favourable substitution of core atoms occurs at the terminal S atom of one monomer motif (0.19 eV), its relative energy being comparable with the position in the staple-like motifs. We can conclude that minimum in energy is related to positions linked to dimer motifs.

(2) We studied a set constituted of 25 isomers when  $n = 2$ , guided by the obtained trend for mono-substitution. Two Ag atoms prefer to incorporate to STF positions, which are attached to dimer and tetramer motifs, but the two isomers with at least one Ag atom located at STF are close in energy (35 meV and 111 meV, respectively). A further analysis of the bonding displayed by the minimum of the  $n = 2$  structure showed that the Au–S (2.55 Å) bond is shorter than the Ag–S bond (2.59 Å) at linkage points of dimer and tetramer motifs. Regarding Au–Ag bonds, it was found that they are comparable to Au–Au bonds, while the two Ag atoms are separated by a distance of 3.02 Å. It is important to mention that when Ag atoms are forming parts of two different staple-like motifs, the relative energy increases to more than 0.26 eV (isomer 19 in Table S1, ESI†), attesting that two Ag atoms substitute core Au atoms preferentially.

(3) A set of 40 isomers was considered for the  $n = 3$  structure. Three Ag atoms located at STF result in a minimum in energy with a calculated HL gap of 1.67 eV. They are attached to both one tetramer (Ag–S bond of 2.56 Å) and one dimer motif (Ag–S bond of 2.60 Å). Calculated Ag–Ag bonds were 3.0, 2.85 and 2.96 Å, which were comparable to the Au–Au bonds of the un-doped cluster. Interestingly, this structure showed similar Ag–Ag, Au–Ag and Au–Au bond lengths.

Moreover, another two isomers held two Ag atoms located at STF with relative energies of 0.14 and 0.17 eV, respectively. Interestingly, two less-stable isomers have Ag atoms in almost parallel triangular faces to the energy minimum, and they are linked either to the monomer motif or to one adatom.

(4) We studied a set of 40 isomers for the  $n = 4$  composition. Four Ag atoms are incorporated into STF plus the special position preferentially (Fig. 2). Another two isomers have been found (29 and 46 meV), which have the STF occupied plus one Ag core atom or one Ag atom located at the monomer motif, respectively. However, when four Ag atoms are substituting adatoms of the tetramer motif, the relative energy is calculated as 0.59 eV. Structurally, the incorporation of four Ag atoms seemed to result in Ag–Au, Au–Au and Ag–Ag bonds comparable in length and dispersed in a range from 2.83 Å to 3.00 Å.

(5) Given the obtained trend in the preference of the Ag doping, we reduce the set of isomers to nine when  $n = 5$ . Substitution of five core Au atoms in the STF results in three isomers which are closely related in energy. The most stable isomer contains, in addition, one Ag atom located at the special position (Ag–S bonds of 2.55 and 2.7 Å) and one core Ag atom linked to one monomer motif (Ag–S bond of 2.52 Å). Another isomer with one Ag atom located at the monomer motif holds a relative energy of 48 meV.

(6) For  $n = 6$ , we considered a set of seven isomers. The minimum in energy maintained the structure of  $n = 5$  plus one Ag atom linked to one monomer motif (Ag–S bond of 2.52 Å). Interestingly, also found was an isomer with three Ag atoms in the STF plus three Ag atoms distributed as follows: one in the special position, one linked to one monomer motif and one incorporated into the monomer motif (5.1 meV). Another isomer (28 meV) contains, in addition, two core Ag atoms linked to the same monomer motif plus one Ag atom substituted in the special position.

(7) In order to confirm the trend in the substitution of silver atoms, in the case of seven silver atoms, we considered a set of 23 isomers. When seven Ag atoms are incorporated in the core, three stable isomers are found. They have relative energies of 0.0, 2.1, and 15.2 meV, respectively. A more stable isomer holds six Ag atoms in the octahedral-like unit, which contains the special position and one Ag atom linked to the monomer motif (Ag–S bond of 2.52 Å). When one Ag atom is located at the monomer motif, the relative energy increases up to 0.143 eV. For the minimum, it was found that Ag–S and Au–S bonds are similar and also one core Au–Au bond was found shorter (2.67 Å) than those Au–Au bonds found in the monometallic cluster.

(8) The number of isomers considered was reduced to three based on the trend obtained for  $n = 7$ . Eight Ag atoms prefer to dope the core, leaving free the atom close to the tetramer motif and linked to one monomer motif. Nonetheless, Ag–Au bonds in the core are clearly distinguished from those bonds linking Au atoms located in the staple motifs and Ag atoms forming the core.

(9) When  $n = 9$ , we considered a set of 11 isomers. A total substitution of the nine core atoms was found to be preferential. The Au<sub>9</sub> core held Ag–Ag bond lengths from 2.77 to 3.2 Å. In contrast, if Ag atoms are part of two monomers and one tetramer motif, the isomer is 0.35 eV less stable. The incorporation of all the nine Ag atoms in the staple-like motifs yielded an isomer with a relative energy of *circa* 1.0 eV.

(10) In order to explore all the preferred sites for Ag doping for  $n = 10$ , we considered 13 isomers. Ten Ag atoms prefer to incorporate to the  $Au_9$  core plus one monomer motif (0.0 eV) or one tetramer motif (8.8 meV). When the Ag atoms are incorporated into two monomer adatoms, one tetramer motif, and  $Ag_7$  core, the relative energy is 0.274 eV.

The obtained trend in the Ag doping is that silver incorporates into atoms of STF and additional atoms prefer to incorporate into either core or adatoms located at monomer motifs ( $n = 4, 5, 6$ ). However, substitution occurs in the inner positions when  $n = 9$ .

All the studied compositions in this report show the presence of one  $Ag_3$  unit located at the middle of the structure (in the triangular face shared by two octahedral-like units). This result is in line with experimental results by Dass *et al.* for crystalline silver doped  $Au_{38}$  cluster.<sup>13a</sup> They attributed the presence of one  $Ag_3$  unit, located at the face shared by two icosahedral units, to the stability conferred to the structure. We think that the combined effects of three monomeric motifs linked across one  $Ag_3$  unit confer stability to the Ag doped  $Au_{18}(SR)_{14}$  structures also.

A further analysis of the calculated HL gaps let us know that the larger value is obtained after substituting seven Ag atoms, and followed by a structure constituted of three Ag atoms, as can be seen in Table 1. However, is important to note that large HOMO–LUMO values are not necessarily related to major stability, as will be shown later.

An important question is related to the relative stability of the doped clusters. In order to know which  $n$  yields the more stable structure, we calculated the energy of the following substitution reactions:



It was found that the lowest substitution reaction energy is obtained when  $n = 2$  with a reaction heat of 0.30 eV (Fig. 4). This result indicates that Ag doping conduces optimal formation of the  $Au_{16}Ag_2(SCH_3)_{14}$  cluster.

It is can be noted that during the revision of this manuscript, the experimental structure of the  $Au_{15}Ag_3(SR)_{14}$  cluster was published.<sup>33</sup> The obtained  $n = 3$  structure seems to contradict the calculated high reaction energy for  $n = 2$ . However, we think that the obtained preference for the  $n = 3$  structure can be ascribed to the high Boltzmann weight (0.98) associated with

**Table 1** Core composition and HOMO–LUMO (HL) gap of most stable  $Ag_nAu_{18-n}(SR)_{14}$  clusters

# Ag atoms	HL, eV
0	1.48
1	1.59
2	1.60
3	1.67
4	1.65
5	1.64
6	1.70
7	1.74
8	1.68
9	1.64
10	1.63

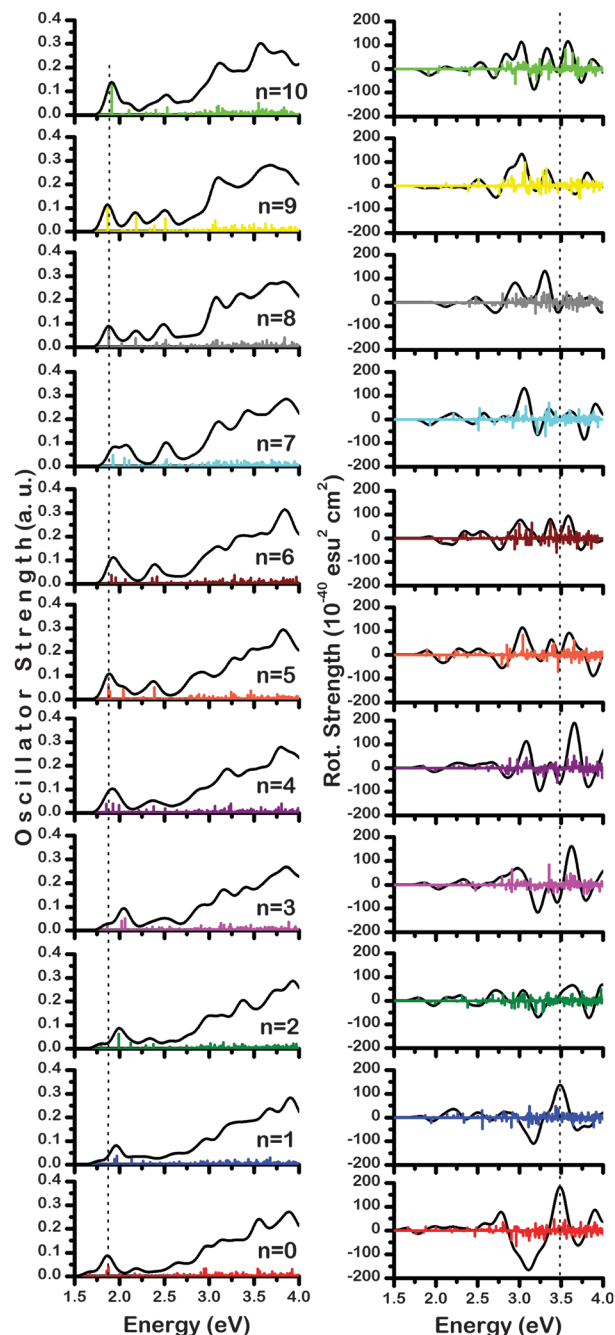


**Fig. 3** Calculated optical absorption (left panel) and CD spectra (right panel) for more stable monometallic and doped clusters;  $n$  indicates the number of Ag atoms. Bottom curve corresponds with the un-doped structure. A Gaussian broadening of 0.15 eV has been used.

the most stable isomer of a set of 40 isomers; while in the  $n = 2$  structure, two isomers showed Boltzmann weights greater than 0.10. Moreover, looking at Fig. 3 and the first intense peak for  $n = 3$ , which is comparable in intensity with the HOMO–LUMO peak of the monometallic cluster (indicated as a dotted line), it is evident that this peak is located at high energy among all studied compositions.

The calculated optical absorption spectrum of the parent thiolated  $Au_{18}$  cluster displays characteristic peaks located at

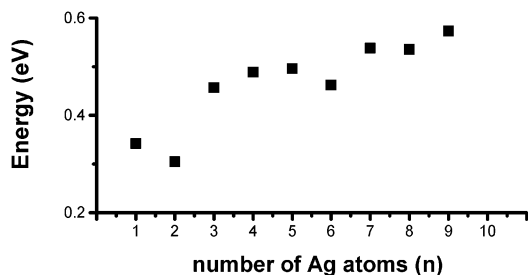


Fig. 4 Energy of the substitution reaction for Ag doping structures. Lowest value indicates the optimal structure.

1.98, 2.18 and 2.75 eV, while the calculated spectrum shows corresponding peaks located at 1.86, 2.17 and 2.64 eV, respectively (Fig. 3, left panel).

Spectral line shapes are qualitatively different for each  $n$ , and new sharp peaks evolve accordingly as the Ag doping increases ( $n > 4$ ); this result coincides with a previous study related to the thiolated  $\text{Au}_{25}$  cluster. However, in the case of the silver doping of the anionic thiolated  $\text{Au}_{25}$  cluster, no enhancement of the oscillator strength was found.<sup>8</sup> In contrast, in this report it is found that starting from four Ag atoms, doped structures show more defined peaks with higher oscillator strengths (*circa* 7.5 times for  $n = 10$ ). Regarding the first peak (HOMO–LUMO transition) found in all spectra, it shifts toward higher energies, with a maximum change of *circa* 0.3 eV for  $n = 3$  (see reported oscillator strengths in Table 2 and Table S2, ESI<sup>†</sup>). This behaviour agrees with the trend obtained in the HL gaps discussed above and shown in Table 1.

The proximity in the relative energies of the calculated isomers may affect the population of possible structures at ambient temperature. We estimate individual contributions by a weighted Boltzmann distribution, in such a manner that the computed intensities of absorption spectra should be

Table 2 First peaks, their oscillator strength, and contribution from HOMO–LUMO transition of studied clusters

# Ag atoms	Peak energy	Oscillator strength	HOMO → LUMO (% contribution weight)
0	1.6671	<b>0.018</b>	85.60
	1.8550	0.047	
1	1.7711	0.015	87.70
	1.9710	0.057	
2	1.7948	0.020	86.00
	1.9912	<b>0.080</b>	
3	1.8633	0.026	79.40
	2.0254	0.042	
4	1.8517	<b>0.043</b>	65.70
	1.9255	0.061	
5	1.8772	<b>0.071</b>	73.60
	1.8944	0.034	
6	1.9095	<b>0.074</b>	56.48
	1.9575	0.042	
7	1.9284	<b>0.075</b>	69.40
	2.0547	0.041	
8	1.8791	<b>0.088</b>	81.90
	2.180	0.059	
9	1.8676	<b>0.114</b>	83.80
	1.9121	<b>0.135</b>	
10	1.9121	<b>0.135</b>	83.30

multiplied by the Boltzmann weight (BW(i)) of each isomer. The number of isomers included in each set for a specific composition  $n$  is included in the denominator of the following formula:

$$\text{BW}(i) = \frac{e^{-E_i/kT}}{\sum_j e^{-E_j/kT}}$$

where  $k$  is the Boltzmann constant ( $8.6173324 \times 10^{-5}$  eV K<sup>-1</sup>),  $T$  is the temperature (298 K), and  $E_i$  is the relative energy of the isomer. Table S1 (ESI<sup>†</sup>) shows the Boltzmann weights and the averaged absorption spectra for isomers of each  $n$ . From Table S1 (ESI<sup>†</sup>), it is concluded that the lowest energy isomers are contributing more significantly to the absorption spectra and mainly to those peaks due to the HOMO–LUMO transitions. For example, for  $n = 3$ , the calculated Boltzmann weight is *circa* 0.99, which means that only the more stable isomer contributes to the absorption spectrum.

On the other hand, a recent study of the enhancement in the fluorescence of a silver-doped rod-shaped  $\text{Au}_{25}$  cluster has been reported by Muniz-Miranda *et al.*<sup>28</sup> They have attributed the enhancement to an intense lower energy peak (large oscillator strength) that is shifted toward high energies in the adsorption spectrum after silver doping. Moreover, they proposed that the fluorescence occurs due to the high oscillator strength of the HOMO > LUMO transitions. It can be noted that several of the silver-doped clusters studied in this report show enhanced peaks related to HOMO > LUMO transitions. For example, by doping with more than four Ag atoms, the first lowest peak of the absorption spectra is intense with respect to the un-doped thiolated  $\text{Au}_{18}$  cluster. Experimental work by Zhou's group has established that the ligand types protecting the thiolated  $\text{Au}_{25}$  core are important because some ligands can enhance the quantum yield.<sup>29</sup> Moreover, the fluorescence mechanism in a thiolated gold cluster is not clear but there exist some important proposals.<sup>30,31</sup>

Regarding chiroptical properties of silver-doped clusters, Jin's group reported that the thiolated  $\text{Au}_{18}$  cluster is non-chiral because there exists a symmetry plane along the dimer motif.<sup>21b</sup> We agree that considering only the Au–S framework could be viable for determining the thiolated  $\text{Au}_{18}$  cluster as non-chiral, but including ligands and their relative orientations (steric hindrance) may change the symmetry. We built a  $C_s$  structure (Fig. S5, ESI<sup>†</sup>) covered with  $-\text{SCH}_3$  as ligand and compared it against the  $C_1$  isomer. Interestingly, the  $C_s$  isomer is 3.06 eV less stable than the  $C_1$  structure. This result indicates that  $\text{Au}_{18}$  protected with  $-\text{SCH}_3$  is chiral, as was previously reported by Tsukuda *et al.*<sup>32</sup> A further comparison of the experimental absorption spectra confirms that Tsukuda's and Jin's groups reported similar UV data (see the comparison on Fig. S3, ESI<sup>†</sup>). Along with this report, we used the Tsukuda CD data of the parent  $\text{Au}_{18}$  cluster for comparison against the silver-doped clusters.

The analysis of the calculated CD spectra suggests the inherent chirality of silver-doped structures. Our results can be summarized as follow:

(1) The CD spectrum of the calculated  $\text{Au}_{18}(\text{SR})_{14}$  features more intense peaks located at 2.79 (+), 2.95 (–), 3.10 (–), and one more intense peak located at 3.49 eV (+) (indicated with a dotted line). The last two peaks coincide with the CD data reported by Tsukuda (Fig. S4, ESI†).

(2) In general, it is observed that silver doping of the thiolated  $\text{Au}_{18}$  cluster results in less intense CD profiles, as can be verified in the right panel of Fig. 3. For example, when one Ag atom is incorporated into the thiolated  $\text{Au}_{18}$  cluster, the obtained CD shows two less intense peaks located at 3.17 (–) and 3.49 (+) eV with respect to the un-doped cluster.

(3) The CD spectrum of the thiolated  $\text{Au}_{18}$  cluster doped with two Ag atoms is similar in the position of peaks included in the range from 3.0 to 4.0 eV, but their intensity is clearly diminished.

(4) Two distinct and positive peaks located at 3.08 and 3.65 eV are found for the  $n = 4$  structure. The profiles of  $n = 3$  and  $n = 4$  are similar in the range from 3.0 to 4.0 eV.

(5) In the case of  $n = 5$  and  $n = 6$ , their profiles display three positive peaks in the range from 3.0 to 3.75 eV, which are comparable in intensity in the case of the  $n = 6$  structure. However,  $n = 5$  has a negative intense peak located at 3.9 eV.

(6) For the  $n = 7$  cluster, a positive and distinct peak is located *circa* 3.06 eV, and two negative peaks are located at 3.21 and 3.78 eV, respectively.

(7) Doping with 8 and 9 silver atoms results in similar CD profiles: both curves present two positive peaks but their intensities are reversed. The  $n = 8$  structure shows the positive intense peak located at 3.3 eV, while  $n = 9$  has the intense positive peak around 3.03 eV.

(8) In the case of the structure doped with 10 silver atoms, the curve shows three positive peaks located at 3.0, 3.33 and 3.58 eV, and one negative peak located at 3.17 eV.

Fig. 3 depicts calculated CD profiles of more stable isomers for each composition. The obtained less intense CD peaks, when the monometallic  $\text{Au}_{18}(\text{SR})_{14}$  cluster is doped, clearly demonstrate that the experimentally observed less intense CD profile of silver-doped  $\text{Au}_{18}(\text{SR})_{14}$  clusters is not related to either the presence of various isomers at each composition or to a cancellation effect as was published by Kobayashi *et al.*<sup>34</sup>

The analysis of calculated adsorption spectra (Fig. 3) support our conclusion that the thiolated  $\text{Au}_{18}$  cluster displays an enhancement of the peaks related to HOMO–LUMO transitions when more Ag atoms are incorporated. Regarding CD intensity, it is found that it varies accordingly with the number of doping Ag atoms, and a less intense peak located at 3.49 eV is displayed for all studied structures.

The importance of this study is that it is based on the enhancement of the lower energy peak (HOMO–LUMO transitions), which is seen as necessary to improve the quantum yield of these structures.

## Conclusions

In summary, in this communication, we carried out a systematic study of a total set of 180 silver-doped structures. The structure

and electronic, optical and chiroptical properties of the silver-doped thiolated  $\text{Au}_{18}$  cluster were studied. It was found that silver-doped clusters show enhanced HL gap values with respect to the parent  $\text{Au}_{18}$  cluster. Moreover, it was determined that when three and seven Ag atoms are incorporated into the structure, large HL gap values are obtained. However, the first intense band for  $n = 3$  is located at high energy in contrast to the  $n = 7$  structure. Our calculations show that Ag doping of the thiolated  $\text{Au}_{18}$  cluster disturbs its optical and chiroptical properties, depending on the specific number of incorporated Ag atoms. Calculated absorption spectra show a lowest energy peak with enhanced oscillator strength for some specific compositions that will represent a challenge to synthesize them in order to let us verify their enhanced properties. Another interesting result is that the CD profile of a silver-doped  $\text{Au}_{18}(\text{SR})_{14}$  cluster is less intense, and the positive intense peak located at 3.49 eV is affected by the incorporation of Ag atoms.

These results can be seen as a manner to enhance the photoluminescence properties where it is necessary to obtain structures with enhanced absorption in the optical region (1.5–3.0 eV).

## Acknowledgements

We acknowledge Prof. Rongchao Jin for providing the experimental structure and absorption spectrum of the thiolated  $\text{Au}_{18}$  cluster and Prof. Tatsuya Tsukuda for the experimental UV and CD spectra data used for comparison. The authors acknowledge the Consejo Nacional de Ciencia y Tecnología and the Dirección General de Cómputo y de Tecnologías de Información y Comunicación of Universidad Nacional Autónoma de México. A. T.-F. acknowledges the support by the grant PRODEP DSA/103.5/15/6797.

## Notes and references

- (a) M. W. Heaven, A. Dass, P. S. White, K. M. Holt and R. W. Murray, *J. Am. Chem. Soc.*, 2008, **130**, 3754–3755; (b) M. Zhu, C. M. Aikens, F. J. Hollander, G. C. Schatz and R. Jin, *J. Am. Chem. Soc.*, 2008, **130**, 5883–5885; (c) T. Dainese, S. Antonello, J. A. Gascón, F. Pan, N. V. Perera, M. Ruzzi, A. Venzo, A. Zoleo, K. Rissanen and F. Maran, *ACS Nano*, 2014, **8**, 3904–3912.
- C. A. Fields-Zinna, M. C. Crowe, A. Dass, J. E. F. Weaver and R. W. Murray, *Langmuir*, 2009, **25**, 7704–7710.
- (a) D.-E. Jiang and S. Dai, *Inorg. Chem.*, 2009, **48**, 2720–2722; (b) K. A. Kacprzak, L. Lehtovaara, J. Akola, O. Lopez-Acevedo and H. Hakkinen, *Phys. Chem. Chem. Phys.*, 2009, **11**, 7123–7129; (c) M. Walter and M. Moseler, *J. Phys. Chem. C*, 2009, **113**, 15834–15837; (d) Y. Negishi, W. Kurashige, Y. Niihori, T. Iwasa and K. Nobusada, *Phys. Chem. Chem. Phys.*, 2010, **12**, 6219–6225.
- H. Qian, D.-E. Jiang, G. Li, C. Gayathri, A. Das, R. R. Gil and R. Jin, *J. Am. Chem. Soc.*, 2012, **134**, 16159–16162.
- (a) M. Zhou, Y. Q. Cai, M. G. Zeng, C. Zhang and Y. P. Feng, *Appl. Phys. Lett.*, 2011, **98**, 143103/1; (b) X. Chen, M. Strange and H. Hakkinen, *Phys. Rev. B: Condens. Matter Mater. Phys.*, 2012, **85**, 085422.

- 6 C. M. Aikens, *J. Phys. Chem. C*, 2008, **112**, 19797–19800.
- 7 A. Tlahuice-Flores, *Mol. Simul.*, 2013, **39**, 428–431; (b) Y. Negishi, T. Iwai and M. Ide, *Chem. Commun.*, 2010, **46**, 4713–4715; (c) E. B. Guidez, V. Mäkinen, H. Hakkinen and C. M. Aikens, *J. Phys. Chem. C*, 2012, **116**, 20617–20624; (d) D. R. Kauffman, D. Alfonso, C. Matranga, H. Qian and R. Jin, *J. Phys. Chem. C*, 2013, **117**, 7914–7923; (e) S. Wang, X. Meng, A. Das, T. Li, Y. Song, T. Cao, X. Zhu, M. Zhu and R. Jin, *Angew. Chem.*, 2014, **126**, 2408–2412.
- 8 A. Tlahuice-Flores, *J. Nanopart. Res.*, 2013, **15**, 1–7.
- 9 C. Kumara, C. M. Aikens and A. Dass, *J. Phys. Chem. Lett.*, 2014, **5**, 461–466.
- 10 (a) Y. Negishi, K. Munakata, W. Ohgake and K. Nobusada, *J. Phys. Chem. Lett.*, 2012, **3**, 2209–2214; (b) S. Yamazoe, W. Kurashige, K. Nobusada, Y. Negishi and T. Tsukuda, *J. Phys. Chem. C*, 2014, **118**, 25284–25290; (c) L. Liao, S. Zhou, Y. Dai, L. Liu, C. Yao, C. Fu, J. Yang and Z. Wu, *J. Am. Chem. Soc.*, 2015, **137**, 9511–9514.
- 11 (a) N. Bhattarai, D. M. Black, S. Boppidi, S. Khanal, D. Bahena, A. Tlahuice-Flores, S. B. H. Bach, R. L. Whetten and M. Jose-Yacamán, *J. Phys. Chem. C*, 2015, **119**, 10935–10942; (b) S. Malola, M. J. Hartmann and H. Häkkinen, *J. Phys. Chem. Lett.*, 2015, **6**, 515–520; (c) N. Kothalawala, C. Kumara, R. Ferrando and A. Dass, *Chem. Commun.*, 2013, **49**, 10850–10852; (d) G. Barcaro, L. Sementa, A. Fortunelli and M. Stener, *Nanoscale*, 2015, **7**, 8166–8167; (e) S. Malola and H. Hakkinen, *J. Phys. Chem. Lett.*, 2011, **2**, 2316–2321.
- 12 (a) A. Tlahuice-Flores, U. Santiago, D. Bahena, E. Vinogradova, C. V. Conroy, T. Ahuja, S. B. H. Bach, A. Ponce, G. Wang, M. Jose-Yacamán and R. L. Whetten, *J. Phys. Chem. A*, 2013, **117**, 10470–10476; (b) V. R. Jupally and A. Dass, *Phys. Chem. Chem. Phys.*, 2014, **16**, 10473–10479; (c) Y. Negishi, C. Sakamoto, O. Tatsuya and T. Tsukuda, *J. Phys. Chem. Lett.*, 2012, **3**, 1624–1628; (d) Y. Chen, C. Zeng, C. Liu, K. Kirschbaum, C. Gayathri, R. R. Gil, N. L. Rosi and R. Jin, *J. Am. Chem. Soc.*, 2015, **137**, 10076–10079.
- 13 (a) C. Kumara, K. J. Gagnon and A. Dass, *J. Phys. Chem. Lett.*, 2015, **6**, 1223–1228; (b) C. Kumara and A. Dass, *Nanoscale*, 2012, **4**, 4084–4086.
- 14 (a) Y. Negishi, W. Kuerashige, Y. Niihori, T. Iwasa and K. Nobusada, *Phys. Chem. Chem. Phys.*, 2010, **12**, 6219–6225; (b) Y. Negishi, K. Igarashi, K. Munakata, W. Ohgake and K. Nobusada, *Chem. Commun.*, 2012, **48**, 660–662.
- 15 H. Qian, D.-E. Jiang, G. Li, C. Gayathri, A. Das, R. R. Gil and R. Jin, *J. Am. Chem. Soc.*, 2012, **134**, 16159–16162.
- 16 (a) Z. Wu, M. Wang, J. Yang, X. Zheng, W. Cai, G. Meng, H. Qian, H. Wang and R. Jin, *Small*, 2012, **8**, 2028–2035; (b) T.-Y. Zhou, L.-P. Lin, M.-C. Rong, Y.-Q. Jiang and X. Chen, *Anal. Chem.*, 2013, **85**, 9839–9844.
- 17 T. Udayabhaskararao, Y. Sun, N. Goswami, S. K. Pal, K. Balasubramanian and T. Pradeep, *Angew. Chem., Int. Ed.*, 2012, **51**, 1–6.
- 18 A. Tlahuice-Flores, *Phys. Chem. Chem. Phys.*, 2014, **16**, 18083–18087.
- 19 D. E. Jiang, S. H. Overbury and S. Dai, *J. Am. Chem. Soc.*, 2013, **135**, 8786–8789.
- 20 A. Tlahuice-Flores, M. Jose-Yacamán and R. L. Whetten, *Phys. Chem. Chem. Phys.*, 2013, **15**, 19557–19560.
- 21 (a) S. Chen, S. Wang, J. Zhong, Y. Song, J. Zhang, H. Sheng, Y. Pei and M. Zhu, *Angew. Chem., Int. Ed.*, 2015, **54**, 3145–3149; (b) A. Das, C. Liu, H. Y. Byun, K. Nobusada, S. Zhao, N. Rosi and R. Jin, *Angew. Chem.*, 2015, **127**, 3183–3187.
- 22 (a) A. Tlahuice and I. L. Garzón, *Phys. Chem. Chem. Phys.*, 2012, **14**, 3737–3740; (b) A. Tlahuice and I. L. Garzón, *Phys. Chem. Chem. Phys.*, 2012, **14**, 7321–7329.
- 23 (a) P. Hohenberg and W. Kohn, *Phys. Rev.*, 1964, **136**, B864–B871; (b) W. Kohn and L. J. Sham, *Phys. Rev.*, 1965, **140**(4A), A1133–A1138.
- 24 J. P. Perdew and Y. Wang, *Phys. Rev. B: Condens. Matter Mater. Phys.*, 1992, **45**, 13244–13249.
- 25 G. te Velde, F. M. Bickelhaupt, E. J. Baerends, C. Fonseca Guerra, S. J. A. van Gisbergen, J. G. Snijders and T. Ziegler, *J. Comput. Chem.*, 2001, **22**, 931–967.
- 26 E. van Lenthe, E. J. Baerends and J. G. Snijders, *J. Chem. Phys.*, 1993, **99**, 4597–4610.
- 27 A. Ghosh, T. Udayabhaskararao and T. Pradeep, *J. Phys. Chem. Lett.*, 2012, **3**, 1997–2002.
- 28 F. Muniz-Miranda, M. C. Menziani and A. Pedone, *J. Phys. Chem. C*, 2015, **119**, 10766–10775.
- 29 S. Wang, X. Zhu, T. Cao and M. Zhu, *Nanoscale*, 2014, **6**, 5777–5781.
- 30 Z. Wu and R. Jin, *Nano Lett.*, 2010, **10**, 2568–2573.
- 31 (a) K. Pyo, V. D. Thanthirige, K. Kwak, P. Pandurangan, G. Ramakrishna and D. Lee, *J. Am. Chem. Soc.*, 2015, **137**, 8244–8250; (b) Y. Yu, Z. Luo, D. M. Chevier, D. T. Leong, P. Zhang, D. Jiang and J. Xie, *J. Am. Chem. Soc.*, 2014, **136**, 1246–1249; (c) K. G. Stamplecoskie and P. V. Kamat, *J. Am. Chem. Soc.*, 2014, **136**, 11093–11099; (d) J. Zheng, C. Zhou, M. Yu and J. Liu, *Nanoscale*, 2012, **4**, 4073–4083.
- 32 T. Tsukuda, H. Tsunoyama and Y. Negishi, in *Metal Nanoclusters in Catalysis and Materials Science: The Issue of Size Control*, ed. B. Corain, G. Schmid and M. Toshima, Elsevier, Amsterdam, 2008, p. 373.
- 33 J. Xiang, P. Li, Y. Song, X. Liu, H. Chong, S. Jin, Y. Pei, X. Yuana and M. Zhu, *Nanoscale*, 2015, **7**, 18278–18283.
- 34 R. Kobayashi, Y. Nonoguchi, A. Sasaki and H. Yao, *J. Phys. Chem. C*, 2014, **118**, 15506–15515.